

Draft version, Presented at the PVSAT-10 conference, 23-25 April 2014, Loughborough, UK

## Spatially and Spectrally Resolved Electroluminescence Measurement System for PV Characterisation

M. Bliss\*, X. Wu, K. Bedrich, T.R. Betts, R. Gottschalg

Centre for Renewable Energy Systems Technology (CREST), School of Electronic, Electrical and Systems Engineering, Loughborough University, Loughborough, Leicestershire, LE11 3TU, UK

\*Corresponding Author Tel.: +44 1509 635327, Fax: +44 1509 635341, Email: M.Bliss@lboro.ac.uk

### Abstract

A system that combines the advantages of fast global electroluminescence (EL) measurements and highly detailed spectral EL measurements is presented. A Si camera-based EL system is used to measure the intensity of radiative recombination of the PV device spatially resolved over its full area. A monochromator-based system is then used to measure localised emission spectra at specific points of interest identified, as such as defects and cracks.

The first measurement results of a mc-Si and an a-Si PV device show good agreement with reported behaviour of such devices and highlight the potential to distinguish between different defect types and reveal performance changes that would be missed using camera-based EL only.

### 1 Introduction

Electroluminescence (EL) imaging of photovoltaic (PV) devices has in recent years become an invaluable tool for both quality control in mass production and in research & development in new devices and materials. EL imaging measures the radiative recombination of the device under test (DUT) under forward bias by using a camera. This can highlight problem areas of a DUT even if it is initially performing as it should by showing minute defects as such as cracks, breaks and shunts. Furthermore, EL measurements can be used to elucidate the spatial distribution of minority carrier lifetime and diffusion length and parasitic resistances [1-3]. The main advantages of this measurement method are that it takes little time, and is non-destructive.

The spectral distribution of the emission is lost during standard EL imaging, but this can provide vital characteristics of the radiative recombination mechanisms. Localised, spectrally resolved EL retains the spectral content of the emitted light from the DUT, but costs measurement time. Even though such measurements are much slower, the additional information is useful for determining the quality and material composition of the solar cell junction. It can also be used to probe non-uniformities in the material composition and differentiate between different defect types that cannot be easily distin-

guished using camera-based EL measurements.

This paper presents part of work at CREST looking into changes in PV device quality during aging. To gain further insight into the processes involved, a spectrally resolved EL measurement system in combination with a camera-based, global EL imaging system (Figure 1) has been developed. The aim of the combined measurement system is to utilise the speed of global EL imaging to identify areas of interest, as such as possible defects, and to measure those specific areas using spectrally resolved EL to extract maximum useful information from the emission.

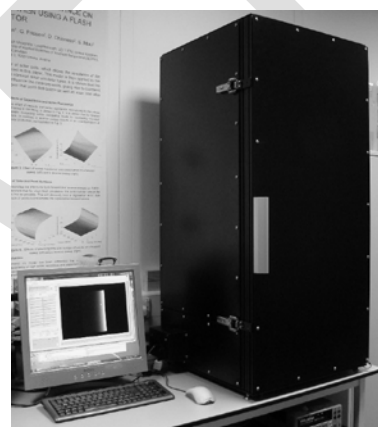


Figure 1: Combined EL imaging and spectral EL measurement system

In the following, the measurement system configuration and applied measurement methods are described in detail. First measurements of a multi-crystalline silicon (mc-Si) and amorphous silicon (a-Si) solar cell are presented and compared against reported behaviour. To conclude, the system optimisation process is discussed.

### 2 Measurement System

#### 2.1 Global EL

Global EL is measured using a 16bit Apogee Alta F-series camera with an 8.3 mega pixel silicon CCD detector. The detector is actively cooled to  $-10^{\circ}\text{C}$  to reduce thermal bias currents and to stabilise the spectral response. Depending on the size of the DUT, different optics are used. Normal optics allow for a better acceptance of light and thus a better signal-to-

noise ratio, while macro optics are used to focus on much smaller samples with a minimum focused image size of 34x26mm giving a resolution of  $\sim 10\mu\text{m}$ . The optics used are without zoom function to maintain good light collection efficiency and short integration times. Instead, the camera is mounted on a guide rail to adjust the distance to the DUT. Filters to reduce effects of unwanted stray light are not used as the enclosure build is light tight, but can be attached to aid particular measurements, for example of diffusion length [2].

To remove the background signal, images are taken with and without sample excitation and subtracted. This also largely reduces the impact of defective bright pixels of the detector, of which the remainders are removed using a 3x3 median filter with threshold applied (i.e. if the pixel value exceeds the median of the surrounding pixels by more than the threshold, its value is set to the median).

## 2.2 Spectrally resolved EL

The system to measure spectral EL emission uses a dual-grating SPEX-270m monochromator with two in-house developed detectors, one Si detector for ultraviolet (UV) to near infrared (NIR) (300-1050nm) and one InGaAs detector for the infrared (IR) (1050-1700nm). The total measurement range is from 0.73eV to 4.1eV. Both detectors are temperature controlled to  $-20^\circ\text{C}$  to reduce noise, stabilise detector spectral response and to reduce thermally induced self-excitation. The photon-induced detector current is internally amplified by a factor 1 billion ( $1\text{E}+9$ ) and measured using a 16bit NI-DAQ card. To further reduce measurement noise and errors in the digitalisation process, the detectors are low pass filtered at  $\sim 3\text{kHz}$  and measured with a 250kHz sampling frequency. The bandwidth of the monochromator has been measured at approximately  $\pm 10\text{nm}$  width half maximum. The optical input for spectral EL is currently a direct fibre coupling to the sample with a measurement spot size of approximately 3mm diameter, albeit development work is ongoing to change this to a microscope-like input with a spot size of  $\sim 100\mu\text{m}$ .

Spectrally resolved EL can be measured using 2 different methods. The first and most commonly used method is the AC mode in which the sample is excited with a forward or reverse current or voltage at a specific rectangular pulse frequency (ranging from 10 to 250Hz). The system utilises a digitally programmed lock-in technique to extract the measurement signal at that specific frequency from the background detector white noise and other signal fluctuations due to external influences. The total noise voltage after a 500ms AC measurement interval is  $\sim 5\mu\text{V}_{\text{rms}}$  (equiva-

lent to 5 fArms). The second method applied is the DC mode in which the device under test is energised using a constant excitation. This makes the measurements more prone to external influences as such as noise, but allows for measuring slow responding devices such as dye-sensitised solar cells.

## 2.3 System Integration

The system is capable of measuring small-area samples, i.e. mini-modules and laboratory samples, of a size of up to 100mm x 100mm. The sample size is currently limited by the peltier-based temperature controlled sample plate. The controller can regulate the temperature of the sample from  $15^\circ\text{C}$  to  $95^\circ\text{C}$  (limited due to the room dew point).

As visible in Figure 2, the light-sealed equipment enclosure additionally houses an XY-stage on which the DUT with the temperature plate is placed. This is used to move the sample between measurements of global EL and localised spectral EL and to change the measurement point during spectral measurements.

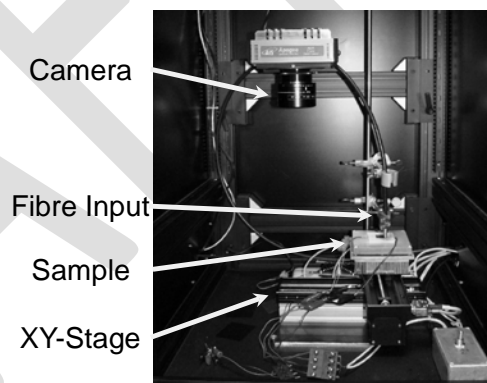


Figure 2: Interior of the measurement system showing sample area, EL camera and spectral EL fibre input

A Keithley 2045 is used as a 4-wire source unit. An additional switching circuit is used to provide the AC square wave excitation for measuring localised spectral EL emissions.

## 3 Initial Measurements

A single cell amorphous Silicon (a-Si) and a multi-crystalline silicon (mc-Si) mini-module device have been measured to test the functionality and as an initial validation of the measurement system.

### 3.1 Multi-crystalline Silicon

The mc-Si device measured is a commercially available mini-module containing 9-cells in series. Its overall size is 60x60mm.

Figure 3 shows the global EL image of the device with an injected current of 100% of the short circuit current ( $I_{\text{SC}}$ ) of the device measured at standard test conditions (STC) and at 20% of the  $I_{\text{SC}}$  value. Note that the emission

profile is more uniform at low excitation current. This is due to the stronger influence of series resistance at high current which induces a high operating voltage shift in the area around the busbars. This large series resistance at the same time reduces the current flow to the areas between the busbars and thus the emitted light due to radiative recombination.

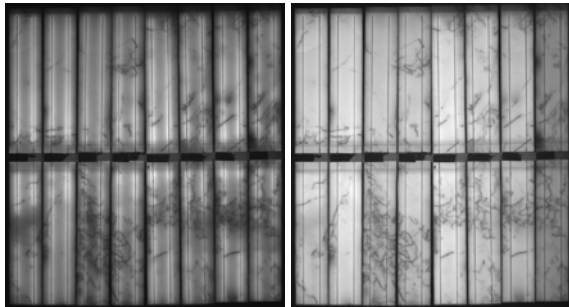


Figure 3: EL images of mc-Si single cell; left: excitation current at  $1xI_{sc}$ ; right: current at  $0.2xI_{sc}$ ; images are normalised, in absolute terms the right image is much darker due to the lower injection current

The darker lines within the cells in Figure 3 that are not straight (i.e. not associated with the busbar and fingers) are difficult to distinguish between intrinsic defects (crystal boundaries) and extrinsic defects (breakage, cracks) using a Si CCD camera. However, by measuring the localised EL emission spectra one can distinguish between them.

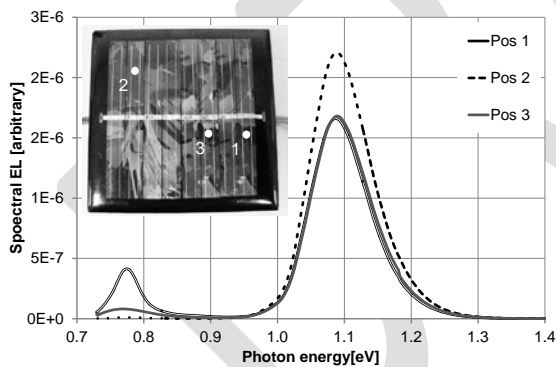


Figure 4: Localised spectral EL measurements of mc-Si sample at different points as indicated

As shown in Figure 4, spectral emission has been measured at three points of interest. All curves show the main emission peak at  $\sim 1.1$  eV or 1150nm. This peak is at the indirect bandgap of c-Si and is consistent with what is reported [4]. Furthermore, one can see a second peak at 0.78eV (1600nm). This peak is identical to what has been reported in [4, 5] and originates from the intrinsic deep traps in the grain boundaries of the silicon crystals. Due to the spectral emission measurement spot being relatively large it was not possible to measure the emission of just the grain defects. Instead the aver-

age emission over a large area (3mm diameter) was measured.

### 3.2 Amorphous Silicon

The a-Si sample measured is a large area laboratory single cell sample with an area of 90x60mm. This cell was chosen as it shows visible discoloration along the cell length. The cell is darker in the middle and less dark on the outer sides, which is a good indicator of non-uniform performance distribution throughout the device.

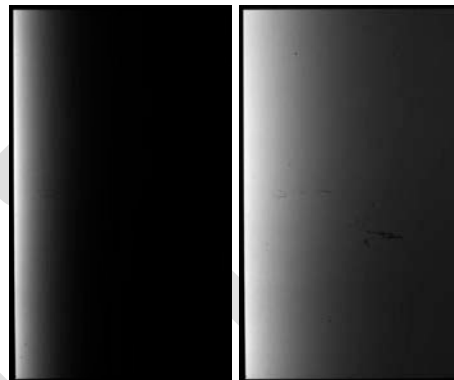


Figure 5: normalized EL images of a-Si cell; left: excitation current at  $1xI_{sc}$ ; right: current at  $0.2xI_{sc}$ ; the bright side of the cell indicates the positive contact

As one would expect from such a large thin-film single cell, it suffers from a significant series resistance loss over the width of the cell between the contacts. Thus, at  $1x I_{sc}$  current injection (left of Figure 5) the signal is very high at the positive side but drops sharply to a very low signal at the negative contact. At  $0.2x I_{sc}$  the signal drop is still visible, but not as strong. Apart from the large series resistance, the cell has a small defect in the low middle part, which is more noticeable in the low excitation current image (right of Figure 5). However, since the global EL intensity distribution is uniform along the length of the cell (top to bottom of Figure 5) changes due to discoloration are not noticeable.

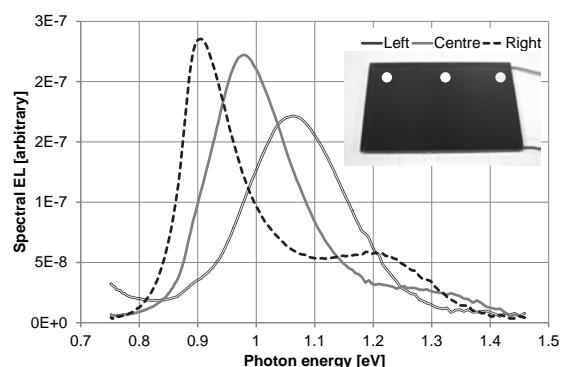


Figure 6: Spectral EL measurements of a-Si sample at different points as indicated

As detailed in Figure 6, the spectral emission of the cell has been measured at points along the positive contact side of the cell. It is noticed that the main spectral emission peak shifts between the measurements on the left to the right of the cell from  $\sim 1.05\text{eV}$  to  $0.9\text{eV}$  ( $1170\text{nm}$  -  $1370\text{nm}$ ). A second peak is visible on the right side emission spectrum at  $1.2\text{eV}$  ( $1040\text{nm}$ ). The emission spectrum is in relative terms almost constant across the width (direction positive to negative contact) of the cell, and only changes in absolute signal strength (results not shown).

The EL emission peak of a-Si is not at its effective band gap which would be at  $\sim 1.55\text{eV}$  (no measurable signals were detected during this work). Instead the dominant recombination and thus the emission peak is at much lower photon energy. In principle the shape of the emission is comparable with reported behaviour of hydrogenated a-Si:H [6, 7]. However, the emission is dependent on many factors as such as temperature, i-layer thickness and material composition (i.e. hydrogen content). At the point of writing the exact cause of the shift in the emission spectrum has not been determined.

To note is that a second sample of the same type, showing no discoloration, was measured and exhibited no change in emission spectrum. This was similar to the right side emission curve in Figure 6.

#### 4 System Development

At the time of writing the system, even though functional, was to some extent still in the optimisation phase. One of the next steps in the project is to change the optical input at the DUT from a direct fibre coupling to a microscope optic. An approximate spot size of  $100\mu\text{m}$  (dependent on wavelength) will ensure that details as such as defects and grain boundaries can be measured accurately. To be able to keep a good signal to noise ratio, the optical efficiency of the monochromator and fibre input will have to be improved at the same time.

The localised spectral response measurements had an initial calibration applied. However, to improve measurement accuracy light spectra as well as linearity will have to be calibrated fully. Nevertheless, the high sensitivity of the detectors makes this a challenging task. Calibration will also have to be applied to the EL imaging camera in the form of uniformity and linearity. This should also correct for the signals of most defective pixels.

Finally, to gain an insight into the measurement uncertainty, the measurements need to be validated with, and compared against other EL imaging and spectrally resolved EL measurement systems.

#### 5 Summary

The set-up of a combined Si-CCD camera-based EL imaging and monochromator-based spectral EL emissions measurement system has been described. Furthermore, details of the next steps in the optimisation of the system are detailed, with the most important improvements being in the optical set-up of the spectrally resolved EL system.

Initial measurements of a mc-Si and a-Si device show a comparable agreement with reported behaviour. This is an important first evaluation step of measurement quality and accuracy and means the system can be used for characterising radiative recombination. Measurement results also highlight the advantage of using a combination of a fast EL imaging technique with detailed EL emission spectrum measurements. Investigating defects and other points of interest is possible with much greater detail and one can further distinguish between different types of defects and gain more information on the material composition and uniformity, details that otherwise might have been missed.

#### Acknowledgements

This work has been supported by a joint UK-India initiative in solar energy through a joint project 'Stability and Performance of Photovoltaics (STAPP)' funded by Research Councils UK (RCUK) Energy Programme in UK (contract no: EP/H040331/1) and by Department of Science and Technology (DST) in India.

#### References

- [1] T. Fuyuki and A. Kitiyanan, " *Applied Physics A*, vol. 96, pp. 189-196, 07/01, 2009.
- [2] P. Würfel, et.al., *J. Appl. Phys.* 101(12), 2007.
- [3] B. Li, et.al., *Prog Photovoltaics Res Appl*, vol. 20, pp. 936-944, 2012.
- [4] T. Fuyuki, et.al., in *Photovoltaic Specialists Conference (PVSC), 2010 35th IEEE*, 2010, pp. 001380-001382.
- [5] K. Bothe, et.al., *Journal of Applied Physics*, vol. 106, pp. 104510-104510-8, 2009.
- [6] K. Wang, et.al., *J. Non Cryst. Solids*, vol. 164-166, Part 1, pp. 595-598, 12/2, 1993.
- [7] D. Han, et.al., *J. Appl. Phys.* 80(4), pp. 2475-2482. 1996.